OPEN ACCESS

ORIGINAL RESEARCH

Intra-aneurysmal hemodynamics: evaluation of pCONus and pCANvas bifurcation aneurysm devices using DSA optical flow imaging

Marta Aguilar Pérez,[1] Hans Henkes,[1] Pierre Bouillot,[2,3] Olivier Brina,[2] Lee-Anne Slater,[4] Vitor Mendes Pereira[4,5]

[1]Klinik für Neuroradiologie, Neurozentrum, Klinikum Stuttgart, Stuttgart, Germany
[2]Interventional Neuroradiology Unit, University Hospital of Geneva, Geneva, Switzerland
[3]Laboratory for Hydraulic Machines (LMH), Ecole Polytechnique Fédérale de Lausanne (EPFL), Avenue de Cour 33bis, CH-1007 Lausanne, Switzerland
[4]Joint Division of Medical Imaging, Department of Medical Imaging, Toronto Western Hospital, University Health Network, Toronto, Ontario, Canada
[5]Division of Neurosurgery, Department of Surgery, Toronto Western Hospital, University Health Network, Toronto, Ontario, Canada

Correspondence to
Dr Vitor Mendes Pereira, University Health Network—Toronto Western Hospital, Division of Neuroradiology, Department of Medical Imaging and Division of Neurosurgery, Department of Surgery, 399 Bathurst Street, 3MCL-436, Toronto, Ontario, Canada M5T 2S8; vitormpbr@hotmail.com, vitor.pereira@uhn.ca

Received 11 August 2015
Revised 30 October 2015
Accepted 2 November 2015
Published Online First 23 December 2015

ABSTRACT

Background Implantation of self-expanding stents from the parent artery into the sac of a bifurcation aneurysm is regularly used to facilitate endovascular coil occlusion with the so-called waffle cone technique (WCT). Self-expanding aneurysm bridging stents like Solitaire AB, can be used; however, bifurcation devices like pCONus and pCANvas are especially designed for WCT. These devices provide additional support for coil implantation owing to intraluminal nylon fibers (pCONus) or membranes (pCANvas) covering the intracranial aneurysm neck.

Objective Assessment of the intra-aneurysmal hemodynamic impact of these three devices: a regular intracranial stent (Solitaire AB) and two bifurcation devices (pCONus and pCANvas).

Material and methods An in vitro experiment was set up using a silicone model of a basilar tip aneurysm filled with blood mimicking fluid under a pulsatile circulation. Solitaire AB, pCONus, and pCANvas were successively implanted in the model for hemodynamic evaluation. High frame rate DSA series were acquired under various conditions. Intra-aneurysmal flow changes, including mean aneurysm flow amplitude ratio (R), were subsequently assessed by the optical flow method, measuring the detector velocity field before and after device implantations.

Results pCONus and Solitaire minimally reduced the intra-aneurysmal flow (R=0.96, p=0.17 and R=0.91, p=0.01, respectively), whereas pCANvas strongly diminished the intra-aneurysmal flow (R=0.41, $p=5\times10^{-12}$).

Conclusions Waffle cone deployment of stents and technique-specific devices had no undesirable effect on the intra-aneurysmal flow. In particular, no increased flow was redirected into the aneurysm sac. The intraluminal membrane of the pCANvas strongly reduced the intra-aneurysmal flow, potentially preventing recanalization problems.

INTRODUCTION

The majority of intracranial aneurysms (IAs) are located at one of the complex bifurcation points of the Willis polygon.[1–4] They often have a wide neck, tend to be more complex than sidewall IAs, and were considered challenging for endovascular treatment before the introduction of intracranial stenting (IS) and bifurcation devices.[3] Depending on the anatomical disposition, it can still be challenging to perform safe treatment of bifurcation IAs with IS. Distal branches with acute angles may be difficult to catheterize or, when achieved, may lead to kinked or flattened stents with significant anatomical and clinical consequences.[5] A new endovascular technique called the 'waffle cone technique' (WCT) was described to overcome this difficulty.[6 7] The WCT consists of placing the intracranial stent in the parent vessel at the level of the neck of the aneurysm without entering the efferent branches of the bifurcation. This technique was described using self-expanding stents,[6–12] originally meant to be deployed in the parent vessel, bridging the aneurysm neck from outside the sac. None of these stents opened distally beyond the physical diameter of the shaft once deployed in the aneurysm.

Recently, dedicated devices for WCT have been developed. The pCONus device (Phenox, Bochum, Germany)[13 14] was optimized for the treatment of bifurcation IAs. It consists of a stent-based support for the proximal vessel with clover-shaped petals creating an effective scaffold for aneurysm coiling reinforced by a net of nylon fibers in the center of the construct to ensure adequate neck support. Initial experiences have shown promising results and technical feasibility.[13 14] An evolution of the pCONus is the pCANvas device with an additional membrane coverage of the petals. It was specifically designed to modify the IA flow in addition to supporting coiling. Indeed, it has been observed that hemodynamics plays an important role in recanalization, thus making evaluation of the effect of these devices important.[30]

To examine this issue, we performed a hemodynamic assessment using high frame rate DSA together with optical flow analysis[15–18] in a controlled in vitro experiment with a patient-specific model of a basilar bifurcation IA. We tested three devices in a WCT configuration: a regular intracranial stent (Solitaire AB) and two bifurcation devices (pCONus and pCANvas).

METHODS

Experimental set-up

A patient-specific silicone model of a basilar tip aneurysm (figure 1) was selected to evaluate the hemodynamic changes inside bifurcation aneurysms in various WCT configurations. After segmentation of the vessel lumen, the model was created using the lost wax method (Elastrat, Geneva, Switzerland). The model consisted of two inlets (vertebral arteries from both distal v2 segments) and two outlets

To cite: Pérez MA, Henkes H, Bouillot P, *et al*. *J NeuroIntervent Surg* 2016;**8**:1197–1201.

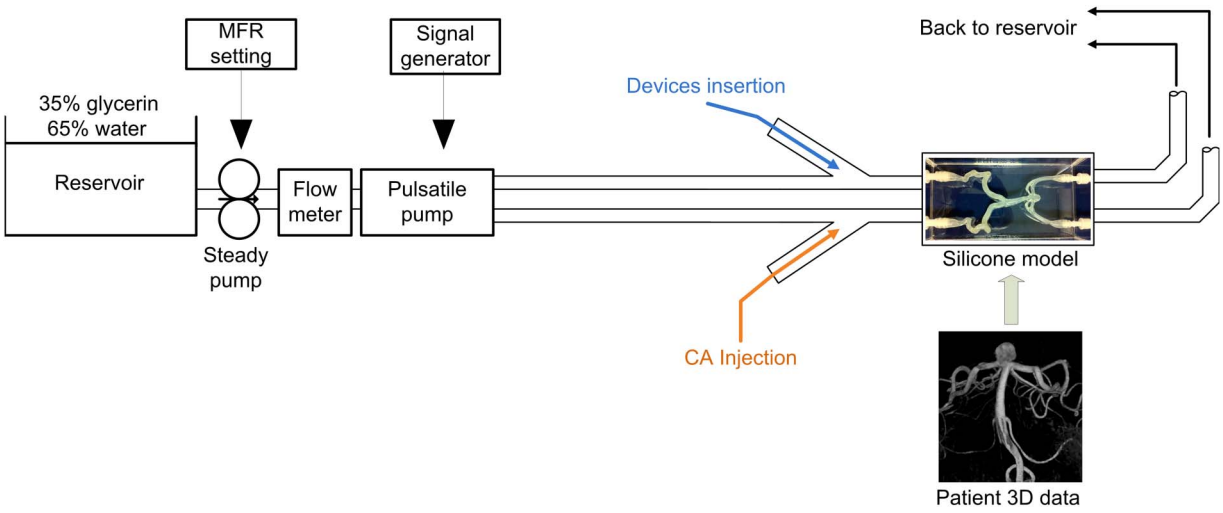

Figure 1 Scheme of the experimental in vitro set-up including a circulating system providing pulsatile flow to a silicone model molded from a patient-specific basilar artery with two inlets. The right vertebral artery was used for imaging while the left one served for device implantations. During imaging acquisitions, the reflux in the left vertebral artery was avoided by clipping. CA, contrast agent; MFR, mean flow rate.

(posterior cerebral arteries merged with superior cerebellar arteries).

The model was connected to an in vitro set-up with a pulsatile circulation. The fluid circulating within the system was a mixture of glycerin (35%) and water (65%) to match the physiological density and dynamic viscosity (1.09×10^{3} kg/m^{3}, 3×10^{-3} Pa.s, respectively, at 20°C) of blood. The fluid was driven through the tubes by a steady pump (Cole Parmer, Vernon Hills, Illinois) at a volumetric mean flow rate of 4.68 cc/s, measured by an electromagnetic flow meter. A 1 Hz temporal variation of the volumetric flow was achieved using a homemade pulsatile piston pump (figure 1). These fluid parameters were similar to previous experimental studies using DSA and optical flow method jointly.[17]

Experiment and device implantation

The two inlets of the silicone model were used to achieve device implantation on one side (implantation access), and contrast agent (CA) injections on the contralateral side (injection access), without disconnecting any tubes from the model during the experiment. The main advantage of this montage is the ability to perform successive device testing without mechanical retrieval maneuvers that might affect the soft silicone model geometry and consequently modify hemodynamic conditions between measurements. For the same reason the devices were not detached, allowing smooth resheathing, and removal from the model. The devices were introduced to the deployment area with their corresponding delivery catheter directly through a 5F introducer sheath placed through the implantation access. After deployment, the delivery catheter was pulled-back and only the wire connected to the device remained in the basilar artery. Three different devices were tested (see figure 2):

1. Solitaire AB (4 mm/20 mm) (Medtronic, Irvine, USA), used regularly in WCT;
2. pCONus (4 mm/25 mm) (Phenox, Bochum, Germany);
3. pCANvas (4 mm/25 mm) (Phenox, Bochum, Germany).

Imaging acquisition

A monoplane angiographic C-arm (Allura FD20, Philips Healthcare, Best, The Netherlands) was used to acquire the imaging data. CA (Iopamiro 300, Bracco; Milan, Italy) was injected from the injection access side of the model using a 5F diagnostic catheter whose tip was placed in the v3 segment. To determine two orthogonal projection views (AP and lateral), a three dimensional (3D) rotational angiography was performed under steady flow conditions.

Then, high frame rate DSA sequences (60 images/s) were acquired in the two projections determined previously, and for each, two different CA injection rates (IRs) were used: 2 and 3 cc/s. These four DSA conditions aimed to assess the influence of both the X-ray projection and the CA injection on the mean aneurysm flow amplitude (MAFA). After each device deployment, these four DSA sequences were systematically acquired with the same exposure (projection view, magnification factor) and CA injection (volume and IR) conditions. The duration of the DSA acquisition was 10 s and was sufficient to cover the wash-in and wash-out of the CA in the aneurysm. It is worth noting that the distal part of the implantation access was clipped at the vertebral level during imaging to avoid back-flow during the acquisition.

Data processing

Flow change analysis, including MAFA, was performed with the flow prototype from Philips Healthcare (Xtravision workstation release V.8.8.1). Pereira *et al* have extensively applied this approach to measure intracranial flow and assess flow diverter stents efficiency.[15–19] An optical flow algorithm was performed on DSA time series to track locally the temporal and spatial CA density variations between the successive images of the run, hence providing the direction and magnitude of the so-called detector velocity fields[18] (DVFs). Figure 3 shows the directions of the DVF as short streamlines superimposed with their magnitude color map. Note that the DVFs do not reflect fully the complex aneurysm flow behavior since absorption of the CA accumulates orthogonally to the projection plane, therefore averaging the CA movement in this direction. However, it provides a valuable indicator of the flow modification between different states.

Flow and statistical analysis

DVF sequences of the three devices (pCONus, pCANvas, and Solitaire AB) were quantitatively compared with the

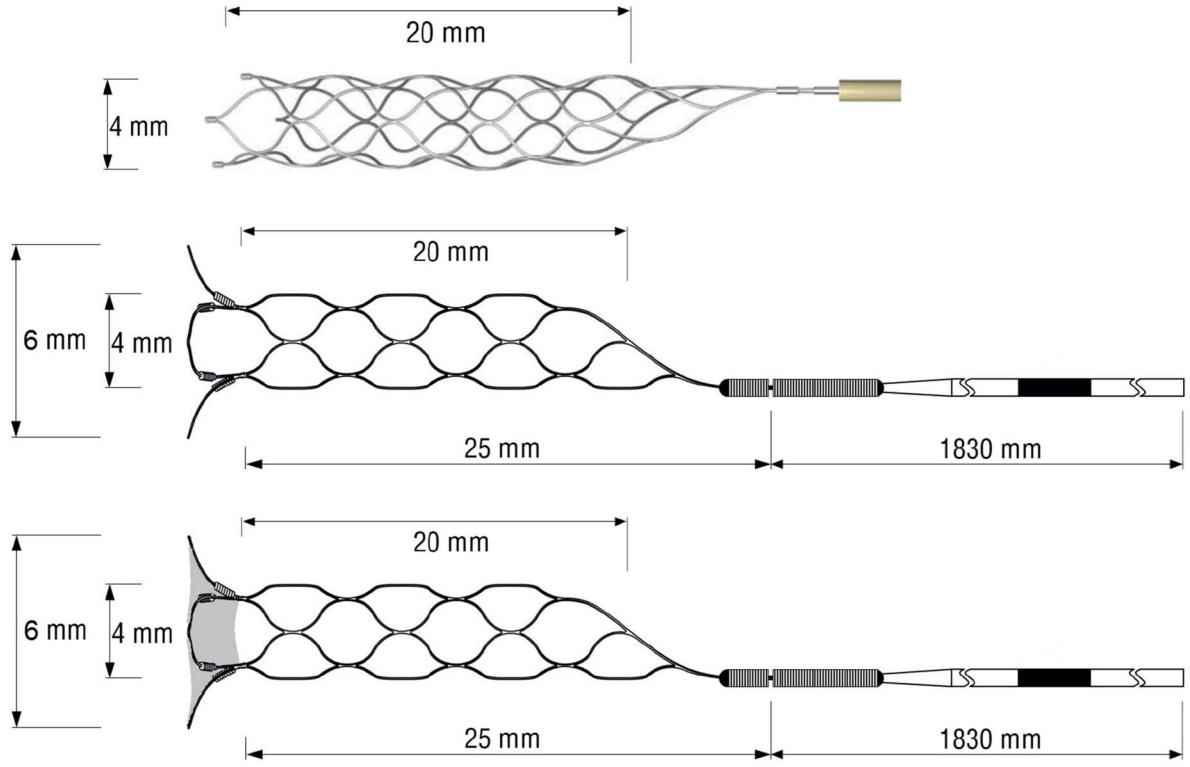

Figure 2 Sketches in lateral view of Solitaire AB, pCONus and pCANvas devices from top to bottom. The pCONus device is based on the structure of a self-expandable retrieval stent. The proximal shaft is similar to a stent. The distal end is made of two crossing intraluminal nylon fibers associated with four distal petals, which are deployed inside the aneurysm sac and rest on the neck circumference stabilizing the device and supporting the coils used to pack the aneurysm. The pCANvas is a derivate of the pCONus device. The design is similar except for the distal end and the petals, which are covered with a membrane offering dense aneurysm neck coverage.

pre-implantation runs. To achieve this, a region of interest surrounding the aneurysm boundaries was defined manually on every dataset (figure 3). Within the region of interest, time and spatial average of the DVF (i.e. MAFA) was therefore computed. The significance of the flow modifications was tested using a Student's t-test based on the four independent DSA runs for each stent implantation. Finally, an estimation of the intra-aneurysmal flow change with the ratio R=MAFApost/MAFApre was calculated for each device based on the average MAFAs.

RESULTS

Device implantations

No technical problems (of navigation and implantation) occurred during delivery of the three devices. In particular, the distal petals of the pCONus and pCANvas devices were deployed in the aneurysm without difficulty and were well apposed to the intra-aneurysmal circumference of the neck orifice. Furthermore, the stent body of the three devices was well apposed against the basilar artery wall. Figure 4, first row,

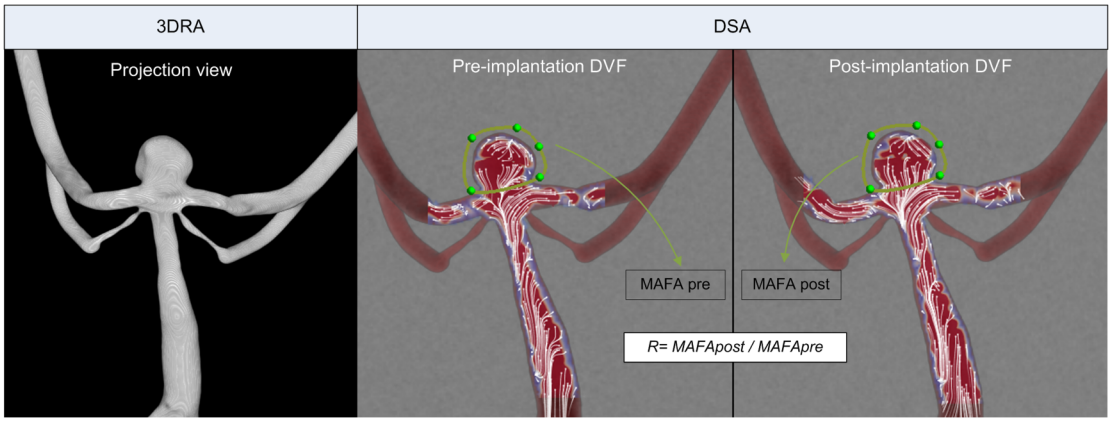

Figure 3 Anteroposterior projection of the three-dimensional rotational angiogram (3DRA) and digital subtraction angiogram (DSA) showing calculation of the mean aneurysm flow amplitude (MAFA) ratio R. Pre- and post-device implantation MAFAs are the time and spatial average of detector velocity fields (DVFs) within the aneurysm region of interest.

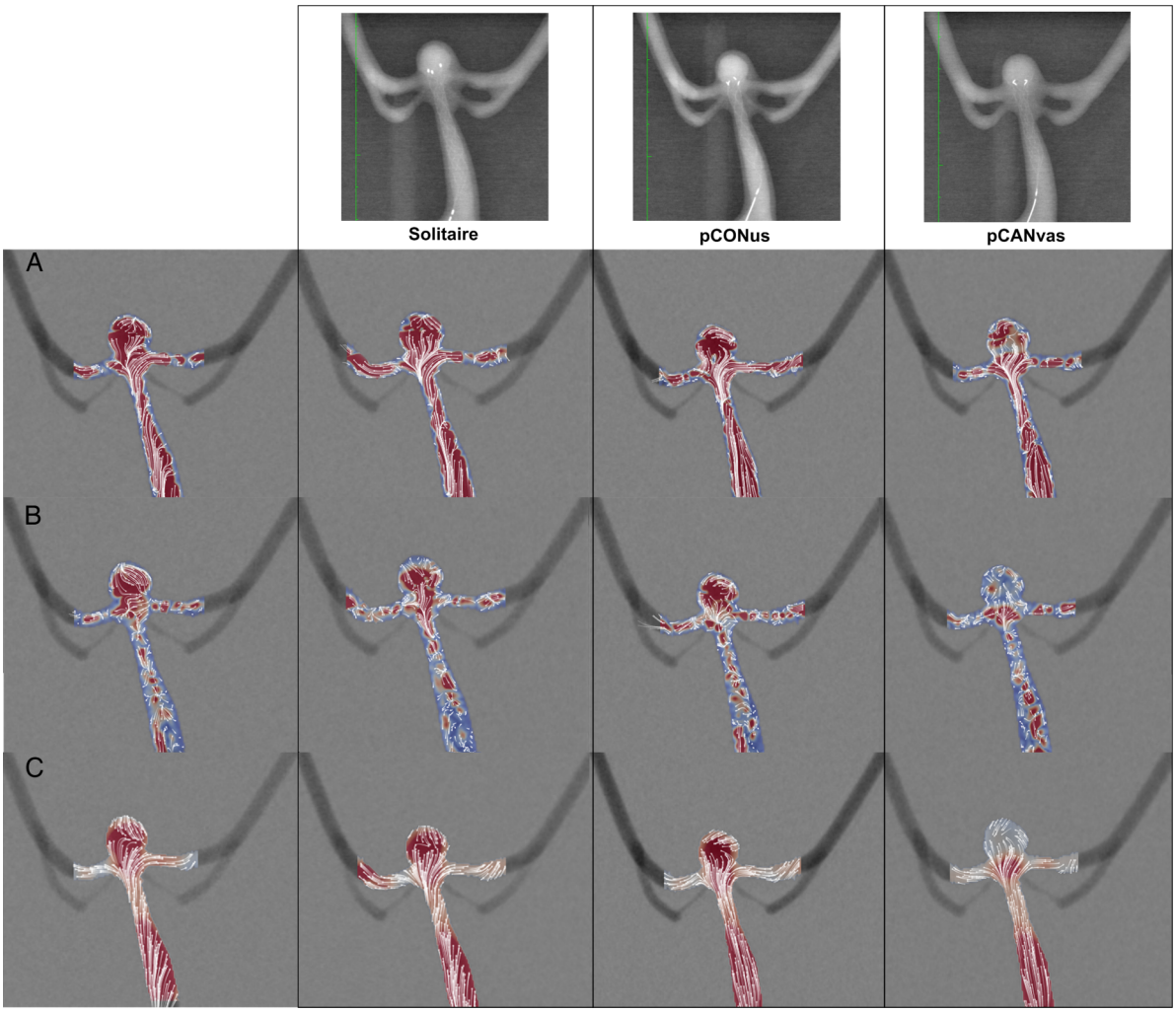

Figure 4 Detector velocity fields (DVFs) displayed as short streamlines (the dot represent the streamline direction) superimposed with a color representation of the velocity magnitude in systolic phase (row A), diastolic phase (row B) of the cardiac cycle; the mean DVF value is shown in row C. The first three columns show the empty state, Solitaire AB and pCONus, respectively, with no visible changes of intra-aneurysmal flow features. Conversely, the strong flow reduction effect of the pCANvas device is particularly visible in the last column.

shows an anteroposterior view of the three devices implanted in the model.

Intra-aneurysmal flow analysis

Intra-aneurysmal flow changes induced by the three devices are summarized in table 1 for the two projections and IRs and in the boxplot (figure 5). For the various DSA conditions, mean (SD) values of MAFA for the empty model, Solitaire AB, pCONus, and pCANvas devices were 6.05 (0.31), 5.80 (0.24), 5.50 (0.39), and 2.45 (0.24), respectively. The low variability of the MAFA values—that is, SDs<10%, shows the reliability and consistency of the measurement despite the various conditions of DSA acquisitions (IR and projection view).

Since pre- and post-devices acquisitions were performed under identical flow conditions, the ratio R reflects the flow changes induced by the implanted device: R>1 corresponds to an increase of the intra-aneurysmal flow after device implantation while R<1 reflects a reduction of intra-aneurysmal flow. On the one hand, low intra-aneurysmal flow reductions were seen for Solitaire AB (R=0.96, p=0.17) and pCONus (R=0.91, p=0.01). On the other hand, the membrane of the pCANvas device induced a high decrease of the intra-aneurysmal flow (R=0.4, $p=5\times10^{-12}$).

In figure 4, DVFs are displayed as short streamlines with a color map representative of the magnitude. The main flow features in diastolic and systolic phases of the cardiac cycle as well as the mean state for the three devices are represented. In particular, the flow modification induced by pCANvas is highlighted by the reduction of the DVF magnitude, especially in the diastolic phase. The two other devices, pCONus and Solitaire AB, with R close to 1, show no visible DVF differences from the empty model, confirming their limited impact on intra-aneurysmal flow.

DISCUSSION

Endovascular treatment of bifurcation aneurysms remain challenging, particularly those with wide necks.[20] Many different techniques and devices have been designed to improve endovascular treatment for bifurcation IAs.[21–23] For instance, various stent configurations were described to protect the distal branches and permit coiling of the aneurysm.[21] However, some bifurcation configurations are not appropriate for IS in any form because of the angle or disposition related to the parent arteries. Complications reported with IS in bifurcations IAs with acute angles include stent kinking, distal branch thrombosis, and arterial dissection.[5 21] The WCT was described as an alternative

Table 1 Pre-/post-implantation MAFA together with the ratio R for each tested device and all acquisitions

Device	Projection	IR	MAFApre	MAFApost	R
Solitaire AB	AP	2	6.20	6.00	0.97
	AP	3	6.00	5.70	0.95
	Lateral	2	5.90	5.50	0.93
	Lateral	3	6.90	6.00	0.87
pCONus	AP	2	6.10	6.00	0.98
	AP	3	5.90	5.60	0.95
	Lateral	2	5.90	5.10	0.86
	Lateral	3	6.10	5.30	0.87
pCANvas	AP	2	6.10	2.60	0.43
	AP	3	6.00	2.70	0.45
	Lateral	2	5.90	2.20	0.37
	Lateral	3	5.60	2.30	0.41

AP, anteroposterior; IR, injection rate; MAFA, mean aneurysm flow amplitude.

to the different stent configurations that require crossing the aneurysm neck and selective catheterization of one or both of the distal branches. It was initially performed with the Neuroform stent (Stryker Neurovascular) and subsequently reported using other stents, including Enterprise, Leo, and Solitaire AB.[6–12 24–29] Designed specifically for WCT, the pCONus may provide increased support of the neck by petals and nylon fibers that provide better support for coiling and preserve the patency of the distal branches.[14 13] The pCANvas has the same purpose and design as pCONus, with additional polycarbonate urethane membrane coverage of the petals. It was designed to maximize the neck coverage along with distal branch protection promoting the intra-aneurysmal flow reduction.

The limited hemodynamic impact observed for both the pCONus and the Solitaire AB confirmed that there was no adverse increase in aneurysmal flow induced by these two devices. As expected, the membrane of the pCANvas induced a strong intra-aneurysmal flow reduction of about 60% as indicated by the measured R=0.4.

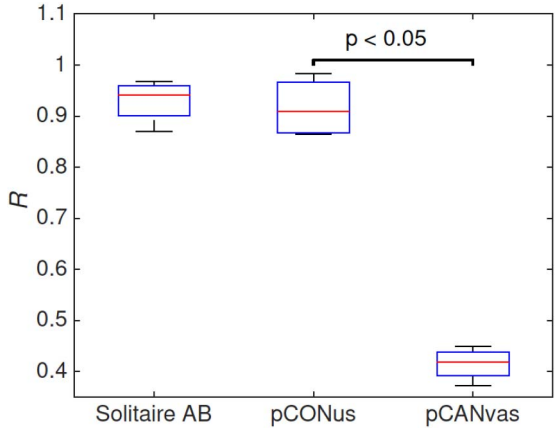

Figure 5 Box plot representation of the mean aneurysm flow amplitude (MAFA) ratio R for the three devices: Solitaire AB, pCONus, and pCANvas. On each box, the central mark corresponds to the median, the edges of the box are the 25th and 75th centiles, and the whiskers extend to the most extreme data points. The measurements errors between four independent acquisitions are low (<10%) within each group. The p value represents the result of the Student's t-test on the flow reduction effect of the device.

From a clinical point of view, the flow diversion effect of the pCANvas is of interest as it may reduce the recanalization rates of coiled bifurcation aneurysm. Luo *et al*[30] observed in a computational study that a high level of wall shear stress and blood flow velocities close to remnant IA necks was associated with future recanalization. The pCANvas could facilitate complete occlusion of the aneurysm sac with optimal packing and protect the neck area from the high flow impingements. These two aspects are essential in preventing recanalization of coiled bifurcation aneurysms. To examine these concerns about recanalization, complementary clinical studies should be conducted to demonstrate the efficiency of the pCANvas.

This study has some limitations. First, the MAFA values were computed on the basis of 2D projections, therefore neglecting the velocity component normal to the detector plane. These results should be confirmed with particle imaging velocimetry (PIV)[31–33] or phase contrast MRI measurements[34] to resolve quantitatively the full 3D velocity fields within the aneurysm cavity. Second, the devices were not delivered and their wires were present in the vessel lumen. This prevented any geometric modifications of the soft silicone model by multiple mechanical retrieval of fully delivered devices and ensured stable flow conditions throughout the experiment required for measurement repeatability.

Even if the optical flow method based on DSA has been used in predicting flow diverter treatment outcomes,[15–18] the method cannot provide actual velocities within the aneurysm cavity. However, we showed in our study that the MAFA ratio was independent of the projection view and CA IR. Furthermore, the significant decrease of R while increasing the impeding material through the neck (two crossing nylon fibers for pCONus and membrane for pCANvas) is consistent. This result confirms that the MAFA ratio is a reliable hemodynamic indicator of relative changes between different states. Additionally, this method is fully applicable to patients intraoperatively.

CONCLUSION

pCONus and Solitaire AB, deployed in WCT, were found to minimally reduce the intra-aneurysmal flow. Conversely, the high flow reduction of pCANvas highlighted its potential in limiting the recanalization concerns of WCT. However, additional clinical and experimental studies assessing 3D velocity fields should be conducted to confirm these findings.

Contributors MAP, HH, and VMP designed and developed the concept of the study. Together with each of the authors, they fulfilled the following criteria: substantial contribution to the acquisition of the data, or analysis and interpretation of the data; draft of the article or revising it critically for important intellectual content; final approval of the version to be published and agree and are accountable for all aspects of the work in ensuring that questions related to the accuracy or integrity of any part of the work are appropriately investigated and resolved.

Competing interests None declared.

Provenance and peer review Not commissioned; externally peer reviewed.

Data sharing statement The authors are willing to share spreadsheets from their data acquisition and experimental set-up details on request.

Acknowledgement We thank our grant agencies: AHSC AFP Innovation Fund and Swiss National Funds - SNF 320030 156813 and SNF 32003B 160222.

REFERENCES

1 [No authors listed]. Unruptured intracranial aneurysms—risk of rupture and risks of surgical intervention. International study of unruptured intracranial aneurysms investigators. *N Engl J Med* 1998;339:1725–33.
2 Bijlenga P, Ebeling C, Jaegersberg M, *et al*. Risk of rupture of small anterior communicating artery aneurysms is similar to posterior circulation aneurysms. *Stroke* 2013;44:3018–26.
3 Pereira VM, Bijlenga P, Marcos A, *et al*. Diagnostic approach to cerebral aneurysms. *Eur J Radiol* 2013;82:1623–32.
4 Pereira VM, Brina O, Gonzalez AM, *et al*. Biology and hemodynamics of aneurysmal vasculopathies. *Eur J Radiol* 2013;82:1606–17.
5 Clarençon F, Piotin M, Pistocchi S, *et al*. Evaluation of stent visibility by flat panel detector CT in patients treated for intracranial aneurysms. *Neuroradiology* 2012;54:1121–5.
6 Yang TH, Wong HF, Yang MS, *et al*. "Waffle cone" technique for intra/extra-aneurysmal stent placement for the treatment of complex and wide-necked bifurcation aneurysm. *Interv Neuroradiol* 2008;14(Suppl 2):49–52.
7 Horowitz M, Levy E, Sauvageau E, *et al*. Intra/extra-aneurysmal stent placement for management of complex and wide-necked-bifurcation aneurysms: eight cases using the waffle cone technique. *Neurosurgery* 2006;58:ONS-258–262; discussion ONS-262.
8 Cho JS, Kim YJ. Modified 'y-configured stents with waffle cone technique' for broad neck basilar top aneurysm. *J Korean Neurosurg Soc* 2011;50:517–19.
9 Guo XB, Yan BJ, Guan S. Waffle-cone technique using solitaire AB stent for endovascular treatment of complex and wide-necked bifurcation cerebral aneurysms. *J Neuroimaging* 2014;24:599–602.
10 Limbucci N, Nappini S, Renieri L, *et al*. Hybrid y stenting with the waffle-cone. A technical note. *Interv Neuroradiol* 2014;20:677–85.
11 Park HR, Yoon SM, Shim JJ, *et al*. Waffle-cone technique using solitaire AB stent. *J Korean Neurosurg Soc* 2012;51:222–6.
12 Sychra V, Klisch J, Werner M, *et al*. Waffle-cone technique with Solitaire™ AB remodeling device: endovascular treatment of highly selected complex cerebral aneurysms. *Neuroradiology* 2011;53:961–72.
13 Mpotsaris A, Henkes H, Weber W. Waffle Y technique: pCONus for tandem bifurcation aneurysms of the middle cerebral artery. *J Neurointerv Surg* 2014;6:e51.
14 Aguilar-Perez M, Kurre W, Fischer S, *et al*. Coil occlusion of wide-neck bifurcation aneurysms assisted by a novel intra- to extra-aneurysmatic neck-bridging device (pCONus): initial experience. *AJNR Am J Neuroradiol* 2014;35:965–71.
15 Pereira VM, Bonnefous O, Ouared R, *et al*. A DSA-based method using contrast-motion estimation for the assessment of the intra-aneurysmal flow changes induced by flow-diverter stents. *AJNR Am J Neuroradiol* 2013;34:808–15.
16 Pereira VM, Ouared R, Brina O, *et al*. Quantification of internal carotid artery flow with digital subtraction angiography: validation of an optical flow approach with Doppler ultrasound. *AJNR Am J Neuroradiol* 2014;35:156–63.
17 Bonnefous O, Pereira VM, Ouared R, *et al*. Quantification of arterial flow with digital subtracted angiography (DSA). *Med Phys* 2012;39:6264–75.
18 Brina O, Ouared R, Bonnefous O, *et al*. Intra-aneurysmal flow patterns: illustrative comparison among digital subtraction angiography, optical flow, and computational fluid dynamics. *AJNR Am J Neuroradiol* 2014;35:2348–53.
19 Pereira VM, Brina O, Delattre BM, *et al*. Assessment of intra-aneurysmal flow modification after flow diverter stent placement with four-dimensional flow MRI: a feasibility study. *J Neurointerv Surg* 2014.
20 Yang P, Zhao K, Zhou Y, *et al*. Stent-assisted coil placement for the treatment of 211 acutely ruptured wide-necked intracranial aneurysms: a single-center 11-year experience. *Radiology* 2015;276:619.
21 Kono K, Terada T. Hemodynamics of 8 different configurations of stenting for bifurcation aneurysms. *AJNR Am J Neuroradiol* 2013;34:1980–6.
22 Pierot L, Klisch J, Cognard C, *et al*. Endovascular WEB flow disruption in middle cerebral artery aneurysms: preliminary feasibility, clinical, and anatomical results in a multicenter study. *Neurosurgery* 2013;73:27–34; discussion 34–35.
23 Pierot L, Moret J, Turjman F, *et al*. WEB treatment of intracranial aneurysms: feasibility, complications, and 1-month safety results with the WEB DL and WEB SL/SLS in the French observatory. *AJNR Am J Neuroradiol* 2015;36:922–7.
24 Gruber TJ, Ogilvy CS, Hauck EF, *et al*. Endovascular treatment of a large aneurysm arising from a basilar trunk fenestration using the waffle-cone technique. *Neurosurgery* 2010;67:ons140–144; discussion ons144.
25 Guo X, Chen Z, Wang Z, *et al*. Preliminary experiences of "Waffle cone" technique for the treatment of intracranial aneurysm. *Zhonghua Yi Xue Za Zhi* 2014;94:1346–8.
26 Luo CB, Lai YJ, Teng MM, *et al*. Reverse waffle cone technique in management of stent dislodgement into intracranial aneurysms. *J Clin Neurosci* 2013;20:1306–8.
27 Nas OF, Kacar E, Kaya A, *et al*. Rare use of twin Solitaire® stents in the double waffle-cone technique for endovascular treatment of a wide-necked bifurcation aneurysm. *Interv Neuroradiol* 2015;21:167–70.
28 Padalino DJ, Singla A, Jacobsen W, *et al*. Enterprise stent for waffle-cone stent-assisted coil embolization of large wide-necked arterial bifurcation aneurysms. *Surg Neurol Int* 2013;4:9.
29 Rahal JP, Dandamudi VS, Safain MG, *et al*. Double waffle-cone technique using twin Solitaire detachable stents for treatment of an ultra-wide necked aneurysm. *J Clin Neurosci* 2014;21:1019–23.
30 Luo B, Yang X, Wang S, *et al*. High shear stress and flow velocity in partially occluded aneurysms prone to recanalization. *Stroke* 2011;42:745–53.
31 Bouillot P, Brina O, Ouared R, *et al*. Particle imaging velocimetry evaluation of intracranial stents in sidewall aneurysm: hemodynamic transition related to the stent design. *PLOS ONE 9* 2014;e113762.
32 Bouillot P, Brina O, Ouared R, *et al*. *J NeuroIntervent Surg* 2016;8:309–15.
33 Bouillot P, Brina O, Ouared R, *et al*. Hemodynamic transition driven by stent porosity in sidewall aneurysms. *J Biomech* 2015;487:1300–9.
34 Pereira V, Brina O, Delattre B, Ouared R, Bouillot P, Erceg G., Schaller K., Lovblad K., Vargas M. Assessment of intra-aneurysmal flow modifcation after flow diverter stent placement with four-dimensional flow MRI: a feasibility study. *J NeuroIntervent Surg* 2015;7:913–9.